Journal of Rock Mechanics and Geotechnical Engineering 14 (2022) 377–384

Contents lists available at ScienceDirect

Journal of Rock Mechanics and Geotechnical Engineering

journal homepage: www.jrmge.cn

Full Length Article

Generic creep behavior and creep modeling of an aged surface support liner under tension

D. Guner [a,b,*], O. Golbasi [b], H. Ozturk [b]

[a] Department of Mining & Nuclear Engineering, Missouri University of Science and Technology, Rolla, MO, USA
[b] Department of Mining Engineering, Middle East Technical University (METU), Ankara, Turkey

ARTICLE INFO

Article history:
Received 17 May 2021
Received in revised form
29 September 2021
Accepted 2 December 2021
Available online 20 December 2021

Keywords:
Time-dependent modeling
Thin spray-on liner (TSL)
Burgers model
Creep constitutive model
Stand-up time

ABSTRACT

Polymer-based materials have been motivated to be an alternative support system element in the mining/tunneling industry due to their logistic and geotechnical benefits. Thin spray-on liner (TSL), a term to define the application of the material on the rock surface with a layer ranging from 2 mm to 10 mm in thickness, shows some promising results. TSLs are mainly composed of plastic, polymer, or cement-based ingredients to a certain proportion. This study intends to reveal the time-dependent response of TSL specimens, cured throughout 500 d, under four constant stress levels for stable laboratory conditions. The results were correlated using two interrelated equations to predict the material's service life (creep-rupture envelopes). The proposed correlations offered an insight into both the effective permanent support time and the strain amount at the liner failure. The time-dependent deformation of TSL, whose performance is highly responsive to creep behavior, was obtained so that the design engineers may use the findings to avoid the severe problems of material creep. Experimental data were also used to develop a Burgers (four-element) creep model. Since the liner has a nonlinear time-dependent behavior, creep models were built for each stress level separately. Subsequently, a generic equation was obtained using the nonlinear parametric dependencies. There is a good agreement between the proposed model and the experimental results. The proposed model can be used as a basis for future numerical studies related to the support behavior of aged surface support liners.
© 2022 Institute of Rock and Soil Mechanics, Chinese Academy of Sciences. Production and hosting by Elsevier B.V. This is an open access article under the CC BY-NC-ND license (http://creativecommons.org/licenses/by-nc-nd/4.0/).

1. Introduction

Various support and reinforcement systems are used to improve and sustain the stability of underground excavations (Yang et al., 2017; Shan et al., 2019; Zhang et al., 2019; Komurlu, 2020; Chen et al., 2021). Surface support elements, also known as areal supports, can distribute the rock mass or rock block load in a larger lining area. Sprayed materials (shotcrete and thin spray-on liner (TSL)), wire mesh, grids and straps are considered as areal support elements in metal mines (Thompsonet al., 2012) and coal mines (Qiao et al., 2014). Conventional shotcrete applications in underground openings have brittle behavior intrinsically and have a long-term curing process to arrive at the required mechanical properties.

Sprayed areal supports can operate as an active support element even though the deformation takes place at a scale of a few millimeters (Tannant, 2001). Therefore, they can interact and support the surrounding rocks at the initial phases before the high growth of deformation on the ground reaction curve (Guner and Ozturk, 2018). Meshes, straps and grids are passive support elements and remain inactive until a large displacement on the ground occurs in a way to develop a close reaction between support and ground. Compared with the passive support systems, TSLs may manage to behave as a pro-active support element in cases where millimeter-scale displacements may lead to a jump in the inherent resistive stress values of the liner (Shan et al., 2019). Even though shotcrete can achieve a comparatively higher support resistance in the conditions where squeezing problems or dynamic events of earthquake and blasting activities are severe, TSLs can provide superior support over the full range of rock deformations (O'Donnell and Tannant, 1998). Because most of the TSLs are more flexible and have better adhesion properties than shotcrete. Overall, polymer-

*Corresponding author. Department of Mining & Nuclear Engineering, Missouri University of Science & Technology, Rolla, MO, USA.
E-mail address: dguner@mst.edu (D. Guner).
Peer review under responsibility of Institute of Rock and Soil Mechanics, Chinese Academy of Sciences.

https://doi.org/10.1016/j.jrmge.2021.12.004
1674-7755 © 2022 Institute of Rock and Soil Mechanics, Chinese Academy of Sciences. Production and hosting by Elsevier B.V. This is an open access article under the CC BY-NC-ND license (http://creativecommons.org/licenses/by-nc-nd/4.0/).

based surface support liners have an encouraging potential in underground operations with their ductile and fast-curing behaviors.

The general definition of TSL is "*cement, latex, polymer-based, reactive or non-reactive, multi-component materials applied to the rock surface sprayed by a nozzle, in a layer of generally* 6 mm *or less (3–5* mm*) thickness to temporarily* support *the excavation*" (Hadjigeorgiou, 2003). TSLs have gained partial acceptability in mining applications in the recent decade due to their operational benefits (Li et al., 2016). However, the majority of the construction and mining sectors still have some doubts about their long-term performance. Recent studies have presented various numerical, analytical and laboratory outputs under certain constraints to explain the support mechanism of TSLs. It is observed that adhesion and direct tensile strength tests have been more commonly investigated by TSL researchers in laboratory studies (Guner and Ozturk, 2019; Kolapo et al., 2021; Liang et al., 2021). Since tensile strength, elongation capability and adhesive strength properties are crucial to understanding the ability of TSL to hold the loose rock in place, these factors should be regarded when evaluating the TSL performance (Yilmaz et al., 2003). The time-dependent response of TSLs is also considered to be vital by researchers in short to long-term practical applications. According to Villaescusa (2014), the creep behavior of TSL may create a severe problem and is a property that has not been investigated yet. Creep tests are also recommended by Kuijpers et al. (2004) to comprehend the time-dependent behaviors of TSLs in detail. They recommended performing creep tests with the loads with 50% of TSLs tensile strength. Polymer-based products may have a noticeable variation in their mechanical properties depending heavily on the changes in time and temperature. Therefore, a safe and proper design can only be achieved by understanding the long-term behaviors of TSLs. In the literature, early-aged (1–14 d) creep behavior of TSL has been discussed (Guner and Ozturk, 2019). Material properties, including creep, strongly depend on the curing time (Guner and Ozturk, 2019; Ozturk and Guner, 2017), and the dynamic loads may influence TSL after a long-time of its application. In this sense, the time-dependent behavior of an aged TSL may gain importance for a complete understanding of TSL behavior.

The creep behavior of the material under ambient conditions mainly depends on the applied stress levels and the time. The general creep curve consists of three stages named transient (primary), steady-state (secondary), and accelerating (tertiary). In the transient stage, the strain rate ($\dot{\varepsilon}$) decreases with time. This stage tends to occur over a relatively short period at the beginning of the test, and the material has a reversible viscoelastic behavior (Sánchez-Beitia et al., 2018). The creep rate is approximately constant and at the lowest level in the steady-state stage. This stage has the most prolonged duration in the test or life of the component. Finally, the creep rate continually increases in the accelerating stage until the failure (Sánchez-Beitia et al., 2018).

Polymer's creep behavior and creep failure process differ from the other engineering materials in various aspects. At this point, creep failure involves complex and combined interactions in several damage mechanisms such as viscoelastic deformation, primary and secondary bond rupture, shear yielding, crazing with intrinsic and extrinsic flaws, culminating in crack initiation, and growth to final fracture (Spathis and Kontou, 2012).

Various research studies have discussed the creep behaviors of different engineering polymers. McKeen (2014) reviewed some prominent time-dependent laboratory works on polymers and generalized creep performance expectations on different types of polymers. Li and Dasgupta (1993) focused on micromechanical deformation mechanisms in polymers during the creep process. In the study, slippage, dislocation motion, craze yielding, and shear yielding were considered deformation mechanisms. On the other hand, polymeric materials used in engineering applications are generally heterogeneous and rheologically complex (Kolařík and Pegoretti, 2006). According to Liu et al. (2008), macromechanical modeling is required for the practical analysis of engineering polymers. These models consist of mathematical equations correlating strain and stress values at the macrostructural level.

Materials are exposed to different loading directions during field applications. Different methodologies of creep tests have been used to simulate the actual material behavior. Tensile, compressive and flexural tests are commonly used when conducting creep tests in polymer and material engineering. The tensile failure mode is one of the critical design factors to explain the falling or sliding wedges (Espley-Boudreau, 1999; Moreau, 2006). Therefore, the tensile creep test methodology for plastics was followed throughout the laboratory studies in the current research. According to Espley-Boudreau (1999), underground implementations showed that applied TSLs are exposed to either constant diagonal or direct tensile stresses depending on the adhesive strength of the TSL. Large displacements may be observed if the surrounding rock mass has some discontinuities, and the direct tensile failure mode should be considered with a priority in that condition.

The primary objective of this study is to investigate the time-dependent material behavior of the surface support liner independently of curing time and develop Burgers rheological model using experimental data. The creep models were developed for different stress levels. The parameters of the creep models were correlated using nonlinear data analysis to build up a generic model. It is observed from the literature that any rheological modeling of TSL material to explain its viscoelastic behavior has not been studied. In addition, any generic mathematical model capable of explaining nonlinearity in TSL strain and creep behaviors has not been offered previously. The current study intends to fill these gaps in the related research area.

2. Experimental methodology

ASTM D2990-09 (2009) testing methodologies were followed throughout the sample preparation, test set-up and tensile/creep test. The experiments of the current study were performed on a cement-based TSL. Product and company names are undisclosed in this study due to confidentiality. The tested TSL has two main ingredients, i.e. a stabilized resin latex in a liquid form and a powder component that is a hydraulically curing powder based on special cement. Components were mixed with a 2:1 liquid-powder ratio by weight. The 7-d cured tensile strength of tested TSL was obtained as 2.91 MPa. This value is higher than 2 MPa, which is the minimum requirement offered by EFNARC (2008).

During the laboratory studies, all the dog-bone-shaped specimens with a thickness of 4 mm were mixed simultaneously to ensure uniformity. The thickness was determined according to the practical TSL applications in underground openings, generally between 3 mm and 5 mm. Ambient conditions in the laboratory were kept constant at (23 ± 2) °C in the specimen preparation phase and throughout the 500-d curing period. The ambient temperature was maintained to be stable by the central heating system and an air conditioner. The die cutter technique was applied for the preparation of the Type-I specimens. Specimen dimensions can be viewed in Fig. 1.

Tensile tests were conducted under a constant displacement rate of 6 mm/min to determine the tensile strength of the 500-d cured TSL, and the load was measured by an S-type load cell with a capacity of 2500 N. Nine different tensile tests revealed that the ultimate tensile strength of the 500-d cured TSL specimens was 3.7 ± 0.15 MPa. The resultant ultimate tensile strength value was

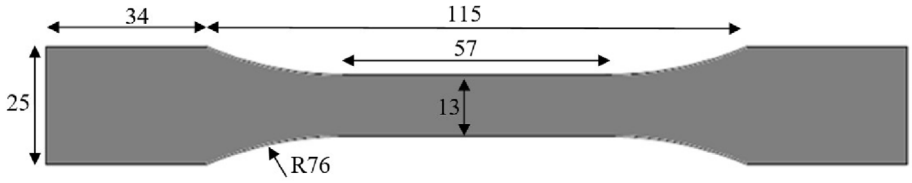

Fig. 1. Dogbone specimen dimensions (in mm).

used to determine the dead weights to be applied in the creep tests. Tensile test results and creep test plans are summarized in Table 1.

At least two specimens should be tested for each stress level, according to ASTM D2990-09 (2009). While laboratory tests were conducted, the attached dead weights were used at the bottom grip (Fig. 2). The top and bottom grips were designed to prevent the sliding of the test specimens. In this way, the eccentric loading of the specimen could also be minimized. Both dial gauges and linear variable differential transformer (LVDT) were mounted to the bottom grips to measure the elongation due to the total forces applied as load and grip weight. A range of dead weights, 80%, 60%, 40% and 20% of the ultimate tensile strength, was applied throughout the experiment. Therefore, these weights induced four different stress levels that are 2.96 MPa, 2.22 MPa, 1.48 MPa and 0.74 MPa, respectively.

3. Test results

The experimental part includes tensile and creep tests conducted at (23 ± 2) °C ambient temperature to examine the relationship between the total strain (sum of elastic and creep deformation) and time. The creep test results are presented in Fig. 3. Depending on the load and failure times ranging from a few minutes to 7 d, the curves that illustrate the total strain versus the time behavior are given in two parts, as shown in Fig. 3. One graph explains the strain behavior for four different stress levels up to 100 min on a linear scale, while the other shows the strain change up to 10,000 min on a logarithmic scale.

As observed from Fig. 3, if a tensile load of 80% of the tensile strength (2.97 MPa) is applied, the failure occurs in 2 min with about 20% strain. On the other hand, the liner can resist for almost 9000 min when the tensile load is applied constantly with a value that is 20% of its tensile strength (0.74 MPa). The elongation capability parameter is inversely proportional to the failure time. As expected, rupture time shows a substantial increase with the decreasing constant load sustained in the specimen. The following section will discuss the statistical correlations between failure time, failure strain and acting stress values.

Table 1
Tensile test results and creep test plan.

Tensile test results		Creep test plan	
Test No.	Ultimate tensile strength (MPa)	Test No.	Applied stress level (MPa)
1	3.55	1	2.96
2	3.71	2	
3	3.63	3	2.22
4	3.49	4	
5	3.74	5	1.48
6	3.61	6	
7	3.75	7	0.74
8	3.95	8	
9	3.9		
Average	3.7 ± 0.15		

3.1. Creep failure analysis

One of the main objectives of this study is to obtain the creep rupture envelope that predicts the load-bearing capability of material under ambient temperature. Creep rupture envelopes are widely used for the service life prediction of polymer-based products. Since a tertiary creep behavior, where rapid acceleration in strain rate exists, is not observed in the laboratory studies, rupture points after the secondary creep are considered in constructing the rupture envelopes. Creep rupture envelopes are plotted based on either stress or strain variation with time considering the critical design parameter. At this point, if the material strain is investigated primarily, a strain versus rupture time curve may be utilized. Otherwise, the graph of stress versus rupture time curve may be chosen. Time dependence of the load-bearing and elongation capacity of the liner were investigated jointly under the scope of this study. Therefore, two creep rupture envelopes, which show a correlation with rupture time, rupture strain and applied stress level (σ_n in MPa), were plotted using nonlinear regression analysis and confidence interval estimation (Fig. 4).

The rupture time (RT) values on the regression line exhibit a continuously descending trend under its reverse correlation with the applied stress, while the maximum cumulative strain where the rupture takes place, $\varepsilon_t(t = RT)$, starts to be stabilized at the stress value higher than 2.5 MPa. Besides, the dashed lines in the graphs show the confidence region where the amounts of $\log_{10}(RT)$ and $\varepsilon_t(t = RT)$ can be estimated with a probability of 95%. The confidence interval estimates on the dependent variable can be performed using Eq. (1). This equation assumes that the estimated value shows a variation regarding the standard error (s) on the dependent variable, $\widehat{Y_0}$, with the critical t value of t-distribution table in a degree of freedom (ν) and an upper tail of $\alpha/2$ for a confidence region of $(1-\alpha)\times 100\%$. In addition to the regression lines, a response surface, which displays the simultaneous interaction of stress, rupture time and strain, was plotted in Fig. 5. If the acting tensile load is known, the plotted rupture envelopes can be used for estimating the effective permanent support time and strain at the rupture of the liner.

$$\widehat{Y_0}_{\min;\ \max} = \widehat{Y_0} \mp t_{\left(\frac{\alpha}{2},\nu\right)} s(\widehat{Y_0}) \tag{1}$$

3.2. Creep behavior modeling of the liner

Time-dependent material models are widely used as approximation techniques to simulate the response of creep strain by stress, time and temperature. In the literature, researchers have generally classified time-dependent modeling in terms of micromechanical or macromechanical approaches. Micromechanical models mainly concentrate on the material behavior on a microscale. On the other hand, macromechanical models, being used to analyze the laboratory outcomes of the tests under simple loads, are considered to identify the material properties. These models are

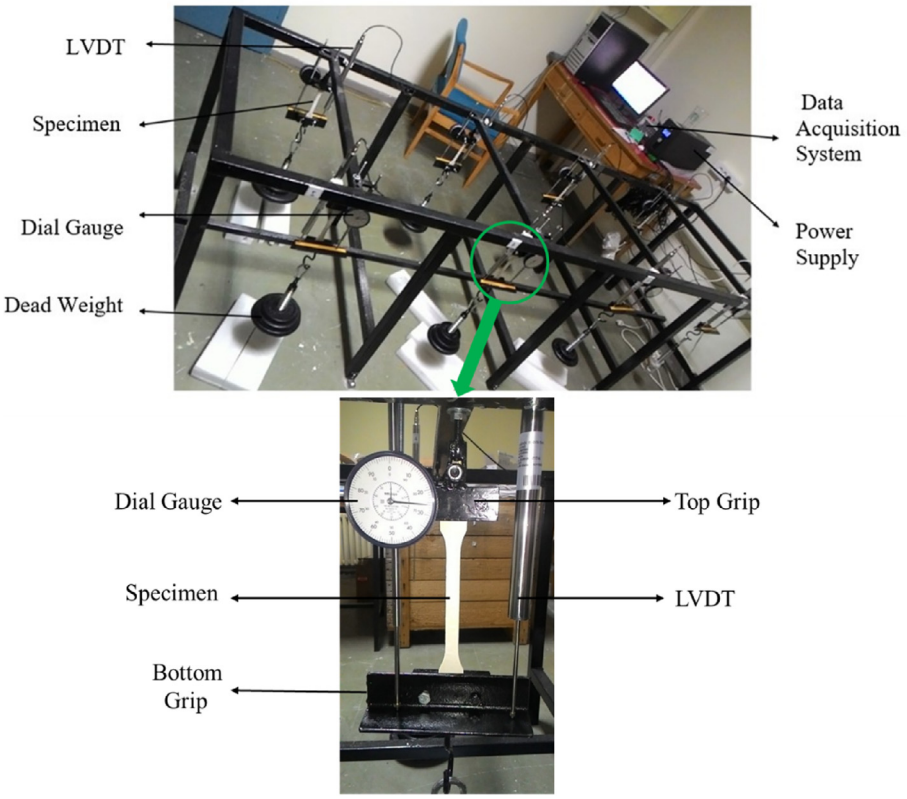

Fig. 2. General view of the testing apparatus.

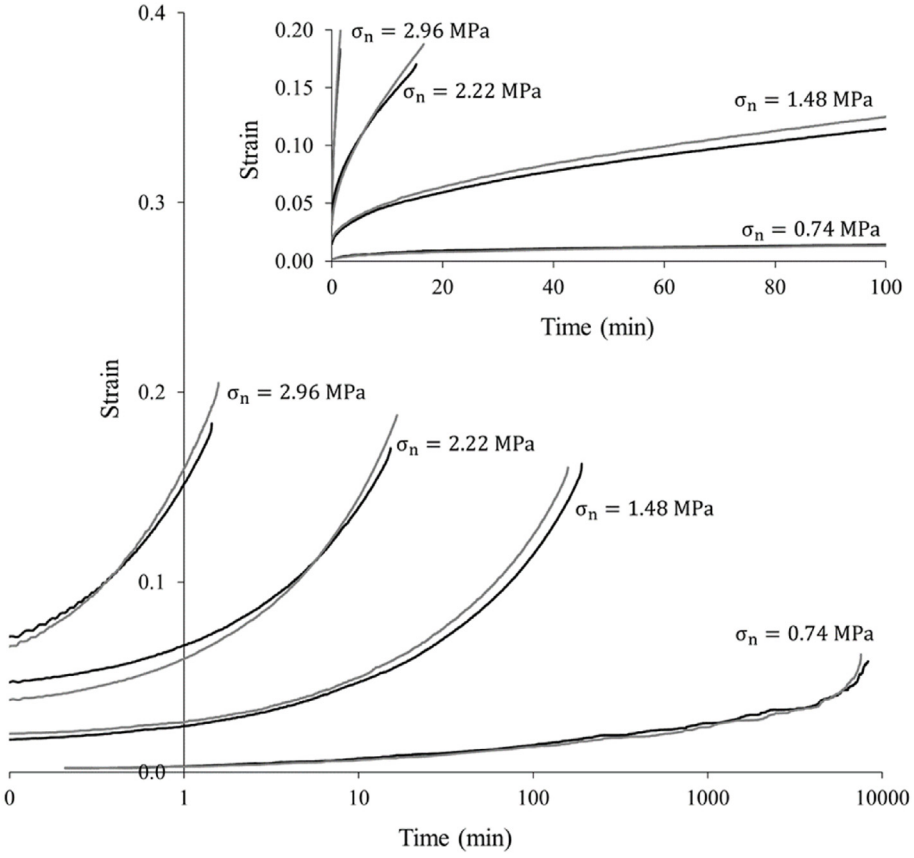

Fig. 3. TSL creep behavior for different stress levels.

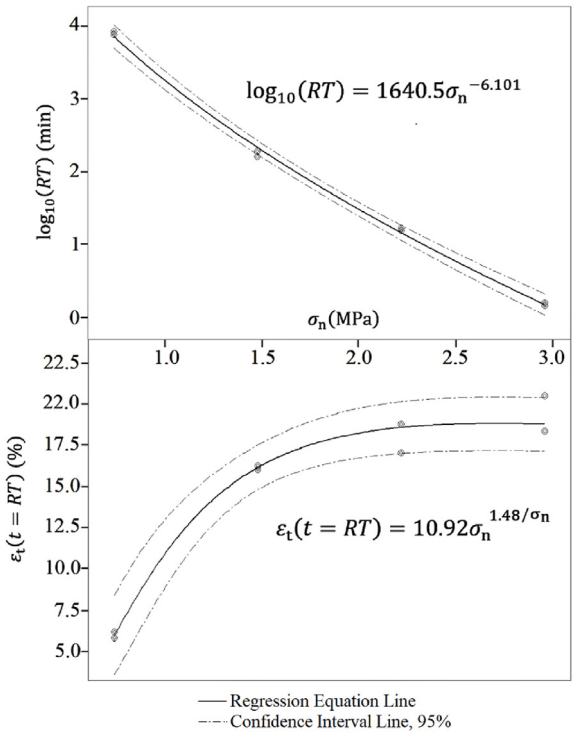

Fig. 4. Correlation between applied stress, rupture time and strain at rupture.

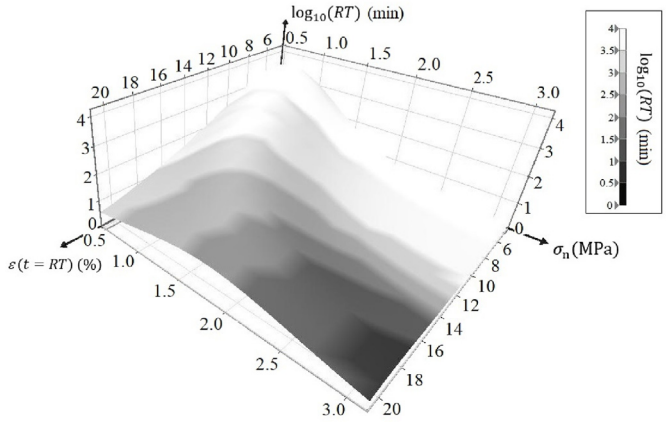

Fig. 5. Rupture time, rupture strain and stress correlation using a response surface.

also used in the mathematical models when highlighting the time-dependent material behavior.

Elastic springs and viscous elements are commonly used to develop a creep behavior model for a time-dependent material. If the tertiary creep is not concerned, the Burgers rheological model offers a practically acceptable simulation of the time-dependent behavior for polymeric materials (Yang et al., 2006). Therefore, this study employs the Burgers rheological model to estimate the general material behavior under constant stress levels. The Burgers rheological model, also called the viscoelastic or four-element model, requires less descriptive parameters when identifying the polymer material parameters (Xu et al., 2017).

The total creep strain is the combination of the instantaneous elastic part of the strain (ε_e) and the viscous time-dependent creep strain function ($\varepsilon_v(t)$). The material strain at a specified time can be expressed with a hereditary integral by Lockett (1972):

$$\varepsilon(t) = \int_0^t \psi(t-\tau)\frac{d\sigma(\tau)}{d\tau}\, d\tau \tag{2}$$

where τ is an arbitrary time (also known as a retardation time) between 0 and t, $\psi(t-\tau)$ is the creep compliance function of the material, and $d\sigma(\tau)/d\tau$ is the stress rate. Since creep tests were performed under uniaxial conditions and the tested stress levels were kept constant, Eq. (2) can be simplified as

$$\varepsilon(t) = \sigma\psi(t) \tag{3}$$

Constitutive equations for the four-element Burgers model can be derived by considering the strain response under the constant stress of a spring, a dashpot, and a Kelvin unit connected in series. Parameters of the Burgers model can be observed from experimental total creep strain-time curves (Fig. 6).

In Burgers model, the creep compliance equation can be defined as

$$\psi(t) = \frac{1}{E_1} + \frac{1}{E_2}\left[1 - \exp\left(-t\frac{E_2}{\eta_2}\right)\right] + \frac{t}{\eta_1} \tag{4}$$

where E_1 is the instantaneous elastic stiffness; E_2 is the elastic modulus of the Kelvin element; and η_1 and η_2 are the viscosities of the Maxwell and Kelvin dashpots, respectively. Burgers model equation can be obtained by substituting Eq. (4) into Eq. (3):

$$\varepsilon_t(t) = \varepsilon_e + \varepsilon_v(t) = \frac{\sigma_n}{E_1} + \frac{\sigma_n}{E_2}\left[1 - \exp\left(-t\frac{E_2}{\eta_2}\right)\right] + \frac{\sigma_n t}{\eta_1} \tag{5}$$

where σ_n is a constant normal stress level.

The nonlinear equation of Burgers model given in Eq. (5) was solved for the stress levels of 2.96 MPa, 2.22 MPa, 1.48 MPa and 0.74 MPa, iteratively. Comparative results between the Burgers model and experimental curves and the generated material constants were presented in Fig. 7 and Table 2, respectively. Solid lines in Fig. 7 refer to the measurement data of the replicated experiments for the individual stress levels, whereas the dashed lines represent the fitted Burger model for the related dataset. It is revealed from the graphs that Burgers model expressed the creep behavior of TSLs for different stress levels very well with a minor standard error (SE) on the fit, which stands for the deviation of the model's line from the actual data.

Statistical correlations between the model parameters in Table 2 were investigated by comparing the standard errors among more than 100 nonlinear equations to determine the best-fitted lines. In addition, the 95% confidence areas were examined to verify whether the values in Table 2 are located between the upper and lower bounds calculated by Eq. (1). The resultant nonlinear expressions correlating the stress levels and parameters E_1, E_2, η_1 and η_2 are given in Fig. 8. It is understood from the graphs that the variations in E_2 values have a direct proportion with σ_n whereas the other parameters exhibit a reverse correlation with the ascending σ_n levels.

Nonlinear equations given in Fig. 8 were substituted in Burgers model (Eq. (5)) to derive a generic model with a single variable σ_n, to generalize the model for different intermediate stress levels. Time-dependent variations of the strain values for the experimental and intermediate stress levels are obtained by Eq. (6), and the resultant creep rupture envelope can be viewed in Fig. 9.

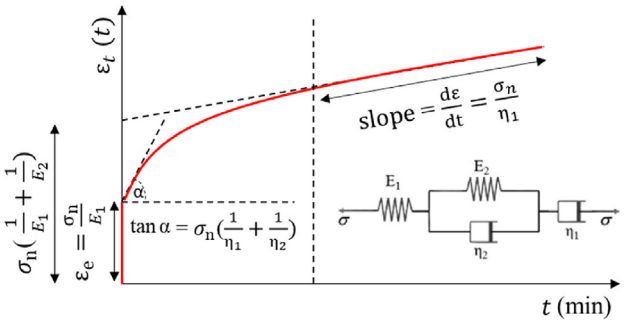

Fig. 6. Burgers model parameters from the curve features and rheological representation.

$$\varepsilon_t(t) = \frac{\sigma_n^{\frac{\sigma_n+2.83}{\sigma_n}}}{173.55} + \frac{\sigma_n^{1-0.277\sigma_n}}{34.59}\left[1-\exp\left(-t\frac{50.12^{\ln\sigma_n}\sigma_n^{0.277\sigma_n}}{50.23}\right)\right] + \frac{426.58^{\ln\sigma_n}\sigma_n t}{32359.36} \quad (6)$$

Fig. 9 shows that the creep curves for intermediate stress levels (red dashed lines) offer a good agreement with the experimental models (black lines). This condition points to the capability of Eq. (6) in estimating the creep behavior for the unknown stress levels successfully. It should be noted that the creep behavior estimations were performed in a stress range between 0.8σ (2.96 MPa) and 0.2σ (0.74 MPa). Therefore, for the stresses smaller than 0.74 MPa, the validity of the given generic equation (Eq. (6)) should be checked with some additional tests.

4. Discussion

The main intention of this study is to highlight and examine the creep behavior of the 500-d cured TSL by performing tensile creep experiments and obtaining a generic constitutive creep model. In the experiments, the testing scenario is motivated to determine the tensile rupturing of a TSL, which is one of the significant parameters when describing the resistance loss of a TSL-lined excavation. Other potential effects based on liner adhesion loss, temperature or humidity variations were not considered under the scope of this study.

The prepared TSLs were molded in the plate, and the specimens were prepared using a die cutter. TSLs are applied on the rock surface by spraying close distances (2–3 m) in field applications. When the bonding characteristics of liner are to be tested in a study, the primary concern is that molded and sprayed materials may behave differently. It is because spraying application positively affects bonding behavior relative to molding. However, the molding and spraying processes have a similar impact on the tensile and creep tests (Guner and Ozturk, 2016).

Laboratory studies showed that the tested aged TSL was highly responsive to the creep. The tested TSL fails within 1 h when the sustained stress level is equal to a value that is half of the TSL tensile strength. Therefore, it is evident that the ultimate tensile strength parameter is not a design parameter for the tested TSL. According to the proposed rupture envelope (Fig. 4), the critical strength limit

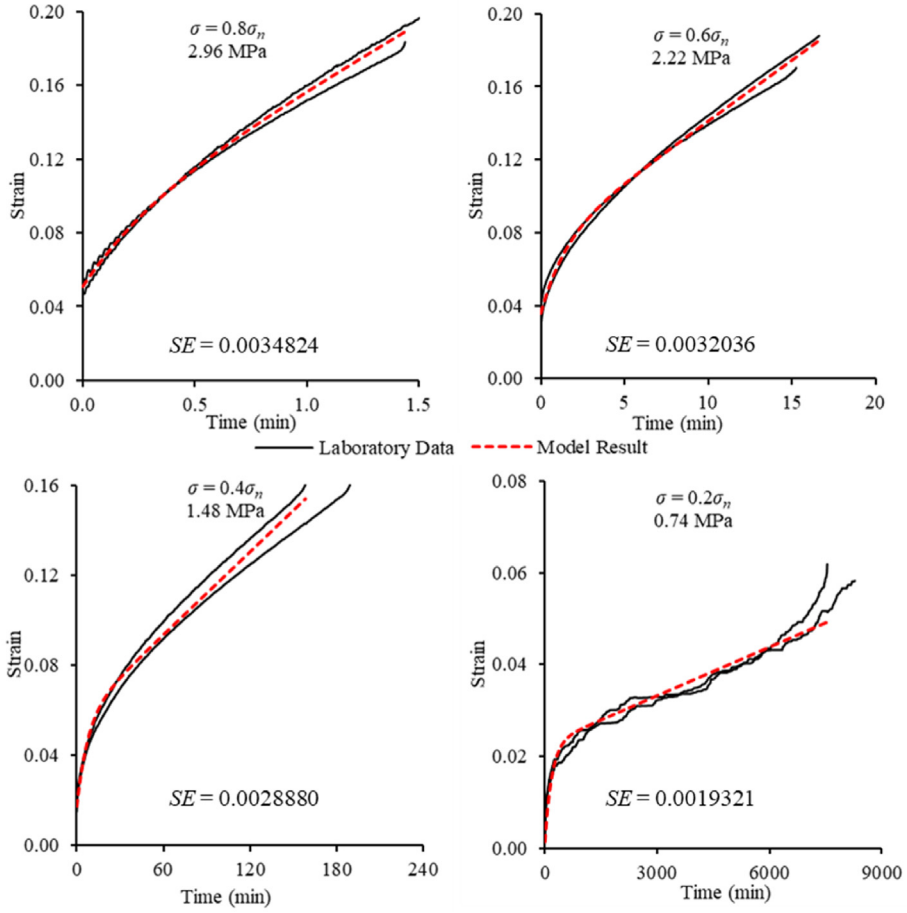

Fig. 7. Comparison of the experimental results and the Burgers model.

Table 2
Time-dependent model coefficients for Burgers model.

Stress level	σ_n (MPa)	E_1 (MPa)	E_2 (MPa)	η_1 (MPa min)	$\log_{10}\eta_1$ (MPa min)	η_2 (MPa min)	$\log_{10}\eta_2$ (MPa min)
0.8 σ_n	2.96	58.1	84.3	41.2	1.6	26.9	1.4
0.6 σ_n	2.22	62.4	57.2	332.4	2.5	84	1.9
0.4 σ_n	1.48	85.5	37.7	2407.3	3.4	288.1	2.5
0.2 σ_n	0.74	548.1	34.8	209,806	5.3	6321	3.8

value for long-term design projects is considered as 10% of the ultimate tensile strength, without considering the other forces such as shear and compression in field applications. The given critical limit for the application of the TSL becomes valid only if the other surface support elements are not combined. It should also be noted that if TSL is combined with stiffer support elements such as shotcrete or wire mesh-shotcrete arrangement, they might prevail the creep of the TSL.

In addition, the creep test results obtained in this study do not imply that TSLs are not practical to be used as an underground areal support element. Surface support materials can distribute the loads on a larger lining area in any field application. For instance, underground wedge blocks can generate minimal stresses on the applied TSL. Let us assume that a regular tetrahedral wedge block exists on the roof in a sliding mode where the side length is about 1 m. Here, the volume of the wedge is calculated as 0.12 m^3. In this case, this wedge can generate only 0.23 MPa tensile stress on the supporting element (liner). According to the given rupture envelope equation in Fig. 4 ($RT = 1640.5\sigma_n^{-6.101}$), TSL can resist this block for more than 20 years. A detailed explanation of calculating the acting tensile stress on TSL can be examined in Guner and Ozturk (2018).

The main objective of the time-dependent modeling part was to develop a generic constitutive creep model of TSL that includes the

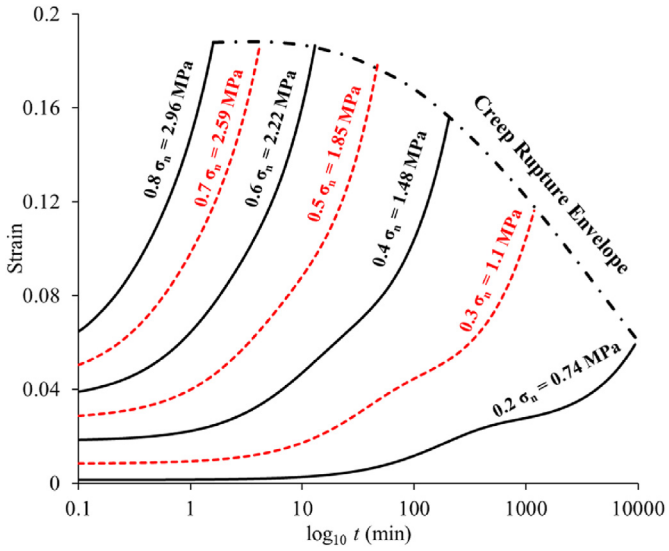

Fig. 9. Derived creep behavior for different intermediate stress levels.

Burgers approach (four-element) for a specific type of TSL. The proposed generic creep behavior model is valid between 0.74 MPa and 2.97 MPa tensile stresses for an aged TSL. The early-age and temporary support performance was not considered in the study scope.

5. Conclusions

This study reveals the statistical dependencies between the acting parameters of the Burgers model using the creep datasets

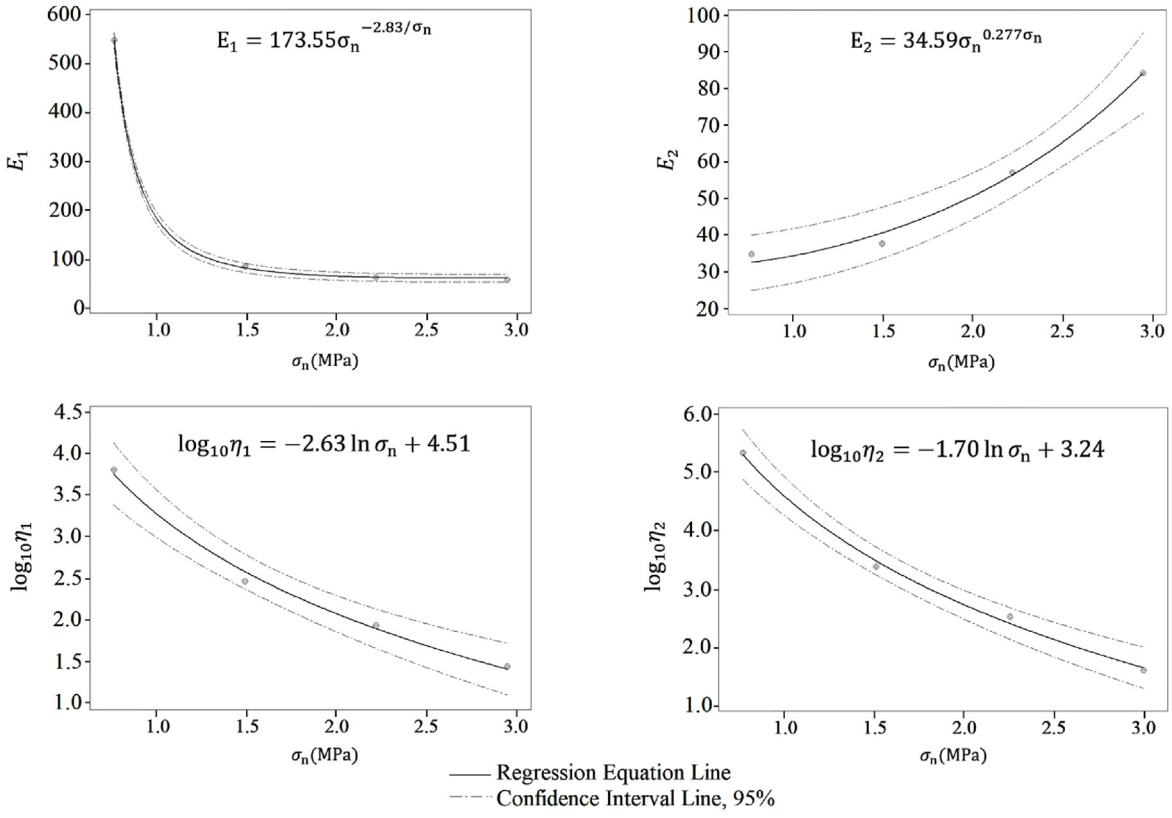

Fig. 8. Variations of acting tensile stress with E_1, E_2, η_1 and η_2.

gathered from laboratory experiments in a controlled ambient condition. In this sense, the liner was exposed to some tensile tests for determining the tensile strength values of the 500-d cured specimens. The test outcomes were used to set the constant stress levels applied in the creep test. It was observed from the creep tests that the liner exhibits a time-dependent deformation behavior. The test set-ups, where the tensile stress varies from 20% to 80% of the tensile strength value with a 20% increment, were used separately. The resultant rupture times ranged from 2 min to 9000 min between the highest and lowest stress levels. The experimental outputs were used to draw the rupture envelopes that correlate maximum strain, rupture time and applied stress. In addition, the statistical dependencies between the Burgers model parameters for different stress levels were revealed. The nonlinear parametric correlations were used to generate a generic creep model, which estimates the constitutive behavior of the TSL as a function of stress, strain and time. The ultimate tensile strength parameter is not a design parameter, and support design engineers should be aware that aged liner has a time-dependent material behavior. Therefore, the generic constitutive creep model generated in this study may be practical in deriving input parameters for a numerical model in future studies when explaining liner's support behavior in a better way.

Declaration of competing interest

The authors declare that they have no known competing financial interests or personal relationships that could have appeared to influence the work reported in this paper.

Acknowledgments

The authors would like to thank the Scientific and Technological Research Council of Turkey, TUBITAK (Grant No. 115M581) for financial support.

References

ASTM D2990-09, 2009. Standard Test Methods for Tensile, Compressive, and Flexural Creep and Creep-Rupture of Plastics. ASTM International, West Conshohocken, PA, USA.
Chen, J., Zhao, H., He, F., Zhang, J., Tao, K., 2021. Studying the performance of fully encapsulated rock bolts with modified structural elements. Int. J. Coal Sci. Technol. 8 (1), 64–76.
EFNARC, 2008. Specification and Guidelines on Thin Spray-On Liners for Mining and Tunneling. ENC 250TSL v7.2 25-07-08.
Espley-Boudreau, S.J., 1999. Thin Spray-On Liner Support & Implementation in the Hardrock Mining Industry. MSc Thesis. Department of Mining Engineering, Laurentian University, Sudbury, Ontario, Canada.
Guner, D., Ozturk, H., 2018. Creep behaviour investigation of a thin spray-on liner. Int. J. Rock Mech. Min. Sci. 108, 58–66.
Guner, D., Ozturk, H., 2019. Experimental and modelling study on nonlinear time-dependent behaviour of thin spray-on liner. Tunn. Undergr. Space Technol. 84, 306–316.
Guner, D., Ozturk, H., 2016. Experimental and numerical analysis of the effects of curing time on tensile mechanical properties of thin spray-on liners. Rock Mech. Rock Eng. 49 (8), 3205–3222.
Hadjigeorgiou, J., 2003. Thin spray-on liners, shotcrete, and mesh. In: Proceedings of the 3rd International Seminar on Surface Support Liners, pp. 1–22. Quebec, Canada.
Kolařík, J., Pegoretti, A., 2006. Non-linear tensile creep of polypropylene: time-strain superposition and creep prediction. Polymer 47 (1), 346–356.
Komurlu, E., 2020. High-density polyurethane rigid foam usability as liner support material in rock engineering. Arabian J. Geosci. 13, 1–13.
Kolapo, P., Onifade, M., Said, K.O., Amwaama, M., Aladejare, A.E., Lawal, A.I., Akinseye, P.O., 2021. On the application of the novel thin spray-on liner (TSL): a progress report in mining operations. Geotech. Geol. Eng. 39, 5445–5477.
Kuijpers, J.S., Sellers, E.J., Toper, A.Z., et al., 2004. Required Technical Specifications and Standard Testing Methodology for Thin Sprayed Linings. Technical Report. CSIR Division of Mining Technology.
Li, J., Dasgupta, A., 1993. Failure-mechanism models for creep and creep rupture. IEEE Trans. Reliab. 42 (3), 339–353.
Li, Z., Tenney, J., Chalmers, D., Mitra, R., Saydam, S., 2016. Application of thin spray-on liners to enhance the pre-drained coal seam gas quality. Energy Explor. Exploit. 34 (5), 746–765.
Liang, H., Han, J., Cao, C., Ma, S., 2021. Laboratory study of deformation behaviour of two new reinforcing polymeric TSLs and their potential application in deep underground coal mine. Polymers 13 (13), 2205.
Liu, H., Polak, M.A., Penlidis, A., 2008. A practical approach to modeling time-dependent nonlinear creep behavior of polyethylene for structural applications. Polym. Eng. Sci. 48 (1), 159–167.
Lockett, F., 1972. Non-linear Viscoelastic Solids. Academic Press, San Diego, USA.
McKeen, L.W., 2014. The Effect of Temperature and Other Factors on Plastics and Elastomers. Elsevier.
Moreau, L.H., 2006. Thin Spray-On Liners: Assessment of Support Performance under Dynamic Loading Conditions. PhD Thesis. University of British Columbia, Vancouver, BC, Canada.
O'Donnell, J.D.P., Tannant, D.D., 1998. Field pull tests to measure in situ capacity of shotcrete. In: Canadian Institute of Mining and Metallurgy Annual General Meeting.
Ozturk, H., Guner, D., 2017. Failure analysis of thin spray-on liner coated rock cores. Eng. Fail. Anal. 79, 25–33.
Qiao, Q., Nemcik, J., Porter, I., 2014. Shear strength testing of glass fibre reinforced thin spray-on liner. Géotech. Lett. 4 (4), 250–254.
Sánchez-Beitia, S., Luengas-Carreño, D., de Antonio, M.C., 2018. The presence of secondary creep in historic masonry constructions: a hidden problem. Eng. Fail. Anal. 82, 315–326.
Shan, Z., Porter, I., Nemcik, J., Baafi, E., 2019. Investigating the behaviour of fibre reinforced polymers and steel mesh when supporting coal mine roof strata subject to buckling. Rock Mech. Rock Eng. 52 (6), 1857–1869.
Spathis, G., Kontou, E., 2012. Creep failure time prediction of polymers and polymer composites. Compos. Sci. Technol. 72 (9), 959–964.
Tannant, D.D., 2001. Thin spray-on liners for underground rock support. In: Proceedings of the 17th International Mining Congress and Exhibition of Turkey, pp. 57–68.
Thompson, A.G., Villaescusa, E., Windsor, C.R., 2012. Ground support terminology and classification: an update. Geotech. Geol. Eng. 30, 553–580.
Villaescusa, E., 2014. Geotechnical Design for Sublevel Open Stoping. CRC Press, London, UK.
Xu, G., Peng, C., Wu, W., Qi, J., 2017. Combined constitutive model for creep and steady flow rate of frozen soil in an unconfined condition. Can. Geotech. J. 54 (7), 907–914.
Yang, J.L., Zhang, Z., Schlarb, A.K., Friedrich, K., 2006. On the characterization of tensile creep resistance of polyamide 66 nanocomposites. Part II: modeling and prediction of long-term performance. Polymer 47 (19), 6745–6758.
Yang, S.Q., Chen, M., Jing, H.W., Chen, K.F., Meng, B., 2017. A case study on large deformation failure mechanism of deep soft rock roadway in Xin'An coal mine. China. Eng. Geol. 217, 89–101.
Yilmaz, H., Saydam, S., Toper, A.Z., 2003. Emerging support concept: thin spray-on liners. In: Proceedings of the 18th International Mining Congress and Exhibition of Turkey, pp. 65–72.
Zhang, C., Pu, C., Cao, R., Jiang, T., Huang, G., 2019. The stability and roof-support optimization of roadways passing through unfavorable geological bodies using advanced detection and monitoring methods, among others, in the Sanmenxia Bauxite Mine in China's Henan Province. Bull. Eng. Geol. Environ. 78 (7), 5087–5099.

Dr. Dogukan Guner gained his MSc and PhD degrees in Mining Engineering from Middle East Technical University, Turkey, in 2014 and 2020, respectively. During his MSc and PhD studies, he mainly focused on the laboratory testing and numerical modeling of thin spray-on liners (TSLs). He is currently a postdoctoral fellow at Missouri University of Science and Technology (MS&T) and lead researcher of the project entitled "Improvement of coal pillar rib rating system using empirical and numerical simulation techniques". He is also contributing to current ground movement monitoring, underground coal rib support and slope stability projects of the MS&T research team.